

pubs.acs.org/JPCA Article

Coordination and Solvation in Gas-Phase Ag⁺(C₂H₂)_n Complexes Studied with Selected-Ion Infrared Spectroscopy

Published as part of The Journal of Physical Chemistry virtual special issue "Emily A. Carter Festschrift".

Antonio D. Brathwaite, Timothy B. Ward, Joshua H. Marks, and Michael A. Duncan*



Cite This: J. Phys. Chem. A 2020, 124, 8562-8573



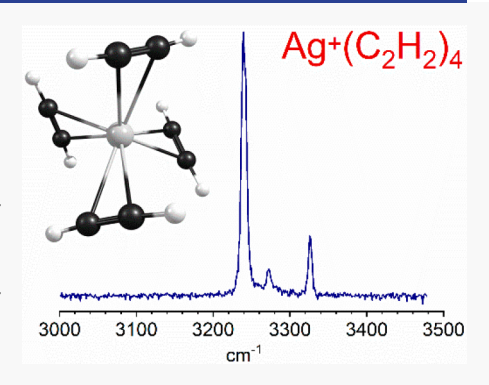
ACCESS

Metrics & More

Article Recommendations

Supporting Information

ABSTRACT: Silver—acetylene cation complexes of the form $\operatorname{Ag}^+(\operatorname{C}_2\operatorname{H}_2)_n$ (n=1-9) were produced via laser ablation in a supersonic expansion of acetylene/argon. The ions were mass selected and studied via infrared laser photodissociation spectroscopy in the C–H stretching region (3000–3500 cm⁻¹). Fragmentation patterns indicate that four ligands are strongly coordinated to the metal cation. Density functional theory calculations were performed in support of the experimental data. Together, infrared spectroscopy and theory provide insight into the structure and bonding of these complexes. The $\operatorname{Ag}^+(\operatorname{C}_2\operatorname{H}_2)_n$ (n=1-4) species are shown to be η^2 -bonded, cation— π complexes with red-shifted C–H stretches on the acetylene ligands. Unlike $\operatorname{Cu}^+(\operatorname{C}_2\operatorname{H}_2)_n$ and $\operatorname{Au}^+(\operatorname{C}_2\operatorname{H}_2)_n$ complexes, which have a maximum coordination of three, silver cation is tetrahedrally coordinated to four acetylene ligands. Larger complexes (n=5-9) are formed by solvation of the $\operatorname{Ag}^+(\operatorname{C}_2\operatorname{H}_2)_4$ core with acetylene. Similar to $\operatorname{Cu}^+(\operatorname{C}_2\operatorname{H}_2)_n$ and $\operatorname{Au}^+(\operatorname{C}_2\operatorname{H}_2)_n$ complexes, acetylene solvation leads to new



and interesting infrared band patterns that are quite distinctive from those of the smaller complexes.

■ INTRODUCTION

Cation $-\pi$ interactions involving transition metals are ubiquitous throughout organometallic chemistry. 1-6 These noncovalent binding forces are important in structural biology, 7-10 and they play pivotal roles in catalytic processes. Transition metal sites in zeolites and metal-organic frameworks (MOFs) have demonstrated enhanced reactivity and selectivity compared to traditional catalysts toward substrates with π -electron systems. ^{14–16} The reactivity of open metal sites in MOFs also makes them promising materials for the storage and separation of gases such as acetylene. 17,18 Accordingly, a clearer understanding of transition metal cation– π interactions is necessary to guide the rational design of new catalysts and materials. Isolated cation-molecular complexes have been studied with mass spectrometry ¹⁹⁻²⁹ and computational chemistry³⁰⁻³⁶ to gain a molecular-level understanding of these interactions. More recently, details on the structure and bonding of metal ion complexes have been revealed via spectroscopy of size-selected complexes.^{37–39} In the present work, we employ similar experimental methods, complemented by density functional theory (DFT) computations, to investigate the structures, coordination, and bonding interactions of gas-phase $Ag^+(C_2H_2)_n$ complexes.

Gas-phase experiments provide favorable conditions that are free from the perturbations of counterions, solvents, and matrices. ¹⁹ Moreover, when combined with computational chemistry, they form a powerful tool to investigate the structure, coordination, and bonding interactions of ion—

molecular complexes. Mass spectrometry has been previously used to obtain insight into the binding energies, fragmentation channels, and reactivity of metal cation— π complexes with one or two ligands. Theoretical studies have also provided information about the electronic structures and geometries of these species, and electronic spectroscopy has revealed details about their preferred bonding configurations and energetics. However, infrared spectroscopy on these and larger species is necessary to obtain structural information. Infrared photodissociation spectroscopy is convenient for studying multiligand complexes because the fragmentation behavior of larger molecules indicates their coordination numbers and, in some cases, identifies products from insertion reactions. Additionally, when combined with theory, this approach can reveal differences in the bonding interactions of coordinating versus solvating ligands.

Our group has previously used infrared spectroscopy to investigate cation— π interactions in metal cation—acetylene and —ethylene complexes. These studies on size-selected complexes have allowed us to systematically investigate the

Received: September 4, 2020 Revised: September 21, 2020 Published: September 25, 2020





bonding interactions of coordinating and solvating ligands. The bonding in these systems is explained by using the Dewar-Chatt-Duncanson 1-6 complexation model. According to this model, acetylene ligands donate π electrons from their HOMO into the σ -type, d orbitals on the metal. The metal also donates electrons from its π -symmetry d orbitals into π^* antibonding orbitals of C₂H₂. Both factors weaken the acetylene bonds and lower its vibrational frequencies. An early study of monoacetylene complexes from our group documented the shifts of the C-H stretches resulting from σ donation and π back-bonding for several first-row transitionmetal cations. 48 In the first work on multiligand complexes, we reported a four-coordinate (4C) tetrahedral structure for the $Ni^+(C_2H_2)_4$ complex. Spectral patterns in larger complexes provided preliminary evidence for an intracluster cyclization reaction; however, no computational studies were available to support the work at that time. 46 In studies on copper and gold, the $Cu^{+}(C_2H_2)_3$, $Au^{+}(C_2H_2)_3$, and $Cu^{+}(C_2H_4)_3$ ions were all found to be cation $-\pi$ complexes with three ligands coordinated directly to the metal cation. For copper and gold cation complexes with acetylene, additional ligands solvated the core M⁺(C₂H₂)₃ ion to form an appealing, highsymmetry $M^+(C_2H_2)_6$ structure.^{49,50} It is interesting to compare the structure, coordination, and bonding of silveracetylene complexes to those of the other coinage metals. Additionally, studies on vanadium cations with multiple acetylene ligands identified the key metallacycle intermediates as well as the reaction product in the cyclotrimerization of acetylene to form benzene. 52 Most recently, we documented the asymmetric coordination, ligand activation, and polymerization of acetylene in complexes with a zinc cation.⁵³ Previously, Krossing and co-workers studied the structures and bonding interactions of $Ag^{+}(C_2H_2)_n$ (n = 1, 3, 4) complexes in solid-state salts with weakly coordinating anions.⁵⁴ In the present work, we employ infrared laser photodissociation spectroscopy to investigate the coordination and solvation of $Ag^{+}(C_2H_2)_n$ (n = 1-7) complexes in the gas phase.

METHODS

 $Ag^{+}(C_2H_2)_n$ and $Ag^{+}(C_2H_2)_nAr_m$ complexes are produced in a pulsed nozzle laser vaporization source by using the third harmonic of a Nd:YAG laser (355 nm; Spectra-Physics INDI) in an expansion of 10% acetylene in argon. The expansion is skimmed into a differentially pumped chamber where positive ions are extracted into a homemade reflectron time-of-flight mass spectrometer. The cluster source⁵⁵ and molecular beam^{56,37} instrument used for these experiments have been described previously. Mass-selected ions were studied with infrared photodissociation spectroscopy by using methods described previously for other metal cation-molecular complexes. 37,58,59 Excitation in the C-H stretching region was accomplished with an infrared optical parametric oscillator/amplifier system (OPO/OPA; Laser Vision, Inc.) pumped by a Nd:YAG laser (Spectra-Physics Pro-230). This OPO provides tunable infrared light in the region of 2000-4000 cm⁻¹ with a line width of about 1 cm⁻¹. Infrared spectra are recorded by monitoring the appearance of one or more fragment ions as a function of the laser frequency. The spectra are not normalized to the laser pulse energy, but the output is nearly constant over the frequency range studied.

Computations were performed in Gaussian09⁶⁰ at the DFT/B3LYP/Def2TZVP level⁶¹ to investigate the structures and

energetics of these complexes. The relative energies presented are zero-point-corrected, and the computed C–H stretching frequencies were scaled by a factor of 0.96 and given a 5 cm⁻¹ FWHM Lorentzian line shape for comparison to the experiment. The 0.96 scaling factor was developed in our previous work on metal ion—acetylene complexes.^{46–53} This brings the computed frequencies for the C–H stretches of acetylene into agreement with the known experimental values.⁶²

RESULTS AND DISCUSSION

A mass spectrum of $Ag^+(C_2H_2)_n$ and $Ag^+(C_2H_2)_nAr$ ions produced by the laser vaporization source is shown in Figure 1.

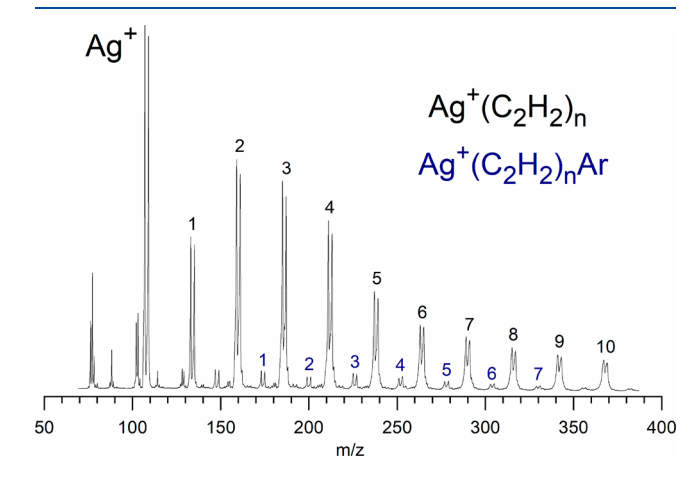


Figure 1. Mass spectrum of $Ag^+(C_2H_2)_n$ and $Ag^+(C_2H_2)_nAr$ complexes.

The peaks are doubled because of the 107 and 109 amu isotopes of silver. The major peaks correspond to $\operatorname{Ag}^+(\operatorname{C}_2\operatorname{H}_2)_n$ ions, whereas minor features result from argon complexes of lighter species. $\operatorname{Ag}^+(\operatorname{C}_2\operatorname{H}_2)_n$ complexes up to n=10 are produced. It is unlikely that all the ligands in larger complexes are coordinated directly to the central silver cation. Instead, these larger ions are likely to be composed of a strongly bound metal—acetylene core, with additional "solvating" ligands attached via electrostatic and/or van der Waals interactions. The solvating ligands in larger complexes should be weakly bound, and efficient ligand elimination is expected for these systems upon IR absorption.

The fragmentation patterns of these complexes following excitation in the C-H stretching region (3000-3500 cm⁻¹) are presented in Figure 2. These data are obtained by subtracting a mass spectrum obtained with the photodissociation laser "off" from one with it "on". The negative peaks indicate depletion of the parent ion, whereas the positive peaks represent the fragment ions produced. Infrared light in the C-H stretching region (3000-3500 cm⁻¹; 8-10 kcal/ mol) does not cause efficient photodissociation of the smaller $Ag^{+}(C_{2}H_{2})_{n}$ complexes (n = 1-3). This is consistent with the relatively high metal ion-acetylene binding energies calculated for these species (see below). Efficient loss of one acetylene ligand is observed for the n = 4 complex. This is not surprising because we calculate the binding energy of acetylene in $Ag^{+}(C_2H_2)_4$ to be approximately 4.6 kcal/mol (1609 cm⁻¹). The loss of two ligands for this species is not expected, and only a small amount of fragmentation is observed for this fragmentation channel. Larger complexes (n = 5-9) undergo

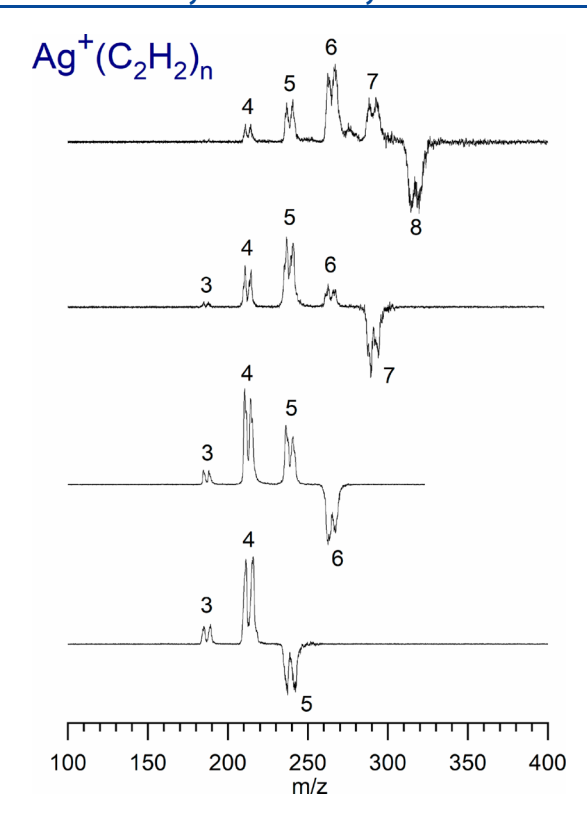


Figure 2. Infrared photodissociation mass spectra of $Ag^+(C_2H_2)_n$ (n = 4-7) complexes.

sequential ligand elimination, terminating at n = 4. Further loss of acetylene is possible but inefficient, as is evident by the weak n = 3 fragment production. This fragmentation behavior suggests that the coordination of Ag^+ is completed with four acetylene ligands. Structural isomers predicted by theory, ligand binding energetics, and vibrational spectra are used to further explore these ideas.

DFT/B3LYP calculations were performed on the singlet and triplet spin states for various $Ag^+(C_2H_2)_n$ and $Ag^+(C_2H_2)_nAr_m$ ions to investigate their structures and energetics. The details of these calculations are presented in the Supporting Information. The structures resulting for the n = 1-4complexes have silver ions interacting with acetylene ligands via an η^2 cation- π configuration, while larger complexes have external ligands. The lowest energy n = 4 complex has a fourcoordinate (4C) nearly tetrahedral structure. A 3C+1 structure is also observed but is predicted to be higher in energy than the 4C structure, and there is no evidence for its presence in our experiment (see below). Two nearly isoenergetic isomers were found for the Ag⁺(C₂H₂)₃ complex. One has a propeller-like structure with D_3 symmetry, and the other has a C_2 structure with slightly higher energy. Although the $Ag^{+}(C_6H_6)$ benzene complex is calculated to lie lower in energy, we do not detect this species in our experiment. No other stable acetylene-based isomers were found for the n = 1-4 complexes; however, isomers involving different attachment sites of argon are identified. The challenges DFT has with weak interactions, such as those involving argon, are well documented. $^{63-65}$ The structures and energetics for argon found here are therefore not expected to be highly accurate. Infrared spectra are presented below with representative structures as insets. Table 1 shows the relative energies obtained for silver cationacetylene complexes, and the binding energies for the

Table 1. Structures, Electronic Ground States, and Relative Energies (Zero Point Corrected) for $Ag^+(C_2H_2)_n$ Complexes Computed by Using DFT/B3LYP; Computed Structures and Energetics from BP86/TZVPP and MP2/TZVPP Theory for $Ag^+(C_2H_2)_3$ Are Also Presented⁵⁴

			*	
,	spin		rel energy	.4
complex	state	symmetry	(kcal/mol)	theory
$Ag^+(C_2H_2)$	singlet	$C_{2\nu}$	0.0	B3LYP
	triplet	C_s	+85.1	B3LYP
$Ag^+(C_2H_2)_2$	singlet	D_{2d}	0.0	B3LYP
	triplet	$C_{2\nu}$	+79.4	B3LYP
$Ag^+(C_2H_2)_3$	singlet	D_3	0.0	B3LYP
	singlet	C_2	+0.1	B3LYP
	triplet	C_2	+81.2	B3LYP
$Ag^+(C_2H_2)_3$	singlet	D_3	0.0	BP86 ^a
	singlet	C_2	+0.24	BP86 ^a
$Ag^+(C_2H_2)_3$	singlet	D_3	0.0	$MP2^a$
	singlet	C_2	+0.48	$MP2^a$
$Ag^{+}(C_{2}H_{2})_{4}$ (4C)	singlet	S_4	0.0	B3LYP
	triplet	C_2	+77.2	B3LYP
$Ag^{+}(C_2H_2)_4 (3C+1)$	singlet	C_2	+0.7	B3LYP
^a Reference 54.				

elimination of either an acetylene or argon from these complexes are presented in Table 2. The acetylene—acetylene

Table 2. Computed Binding Energies (Zero Point Corrected) in kcal/mol for the "Last" Ligand in $Ag^+(C_2H_2)_n$ and $Ag^+(C_2H_2)_n$ Ar Complexes

complex	$E[Ag^{+}(C_2H_2)_{n-1} - C_2H_2]$	$E[Ag^{+}(C_2H_2)_n - Ar]$	$E[Ag^{+}(C_{2}H_{2})$ $Ar-Ar]$
$(C_2H_2)_2$	0.40		
$Ag^+(C_2H_2)$	31.71		
$Ag^{+}(C_2H_2)Ar$ (Ar on Ag^{+})		6.85	
$Ag^{+}(C_2H_2)Ar_2$ (Ar on Ag^{+})			2.43
$Ag^+(C_2H_2)_2$	29.27		
$Ag^{+}(C_2H_2)_2Ar$ (Ar on Ag^{+})		0.57	
$Ag^+(C_2H_2)_3$	8.59		
$Ag^{+}(C_2H_2)_3Ar$ (Ar on CH)		0.50	
$Ag^{+}(C_{2}H_{2})_{4}$ (4C)	4.56		
$Ag^{+}(C_{2}H_{2})_{4} (3C+1)$	3.87		
$Ag^{+}(C_2H_2)_4Ar$ (Ar on CH)		0.38	
$Ag^+(C_2H_2)_5$	3.25		
$Ag^{+}(C_2H_2)_5Ar$ (Ar on CH)		0.29	
$Ag^+(C_2H_2)_6$	2.57		
$Ag^+(C_2H_2)_7$	2.58		

binding in larger complexes can be compared to that of the isolated acetylene dimer. High-level theory computes the binding energy of the CH– π hydrogen bond in the T-shaped dimer to be ~400 cm⁻¹ (1.14 kcal/mol).^{66,67} The binding energies of external ligands are expected to be greater than that of the neutral dimer due to the presence of the charge. However, efficient photodissociation is expected in the C–H stretching region (3000–3500 cm⁻¹). For all species, we find the triplet states to be significantly higher in energy than the corresponding singlets. Additionally, as discussed below and

Table 3. C-H Stretching Vibrational Frequencies (in cm⁻¹) Computed (Scaled by 0.96) for Singlet States of Ag⁺(C₂H₂)_v $Ag^{+}(C_{2}H_{2})_{\mu}Ar$, and $Ag^{+}(C_{2}H_{2})Ar_{2}$ Complexes along with Those Measured in the Experiment^a

•	•	_	•		_		
species	experiment	theory	assignment	species	experiment	theory	assignment
$Ag^+(C_2H_2)$		3200(239)	asym str		3246	3252(132)	core ligand asym str
		3292(7)	sym str		3262	3261(118)	ext ligand asym str
$Ag^{+}(C_2H_2)Ar$	3204(229)	asym str		3310	3318(9)	oop donor sym str	
		3296(11)	sym str			3320(4)	ip donor sym str
0 (2 2) 2	3209/3227	3209(214)	asym str		3326	3333(10)	core ligand sym str
	3296	3300(12)	sym str	$Ag^+(C_2H_2)_6$	3193	3193(306)	double-donor asym
$Ag^+(C_2H_2)_2$		3211(415)	ip/oop asym str				str
		3301(33)	oop sym str		3210	3213(311)	donor asym str
$Ag^{+}(C_2H_2)_2Ar$ 3213/	3213/3239	3212(208),	ip and oop asym str		3216	3219(293)	donor asym str
		3213(212)			3244	3252(130)	core ligand asym str
	3299	3302(28), 3304(2)	ip and oop sym str		3263	3261(102), 3262 (128)	ext ligand asym str
$Ag^{+}(C_2H_2)_3$		3233(148), 3234(349)	ip and oop asym str		3312	3293(17)	double-donor sym str
		3324(36)	oop sym str		3332	3321(10)	donor sym str
$Ag^{+}(C_{2}H_{2})_{3}Ar$ 3230	3230/3252	3230(64),	ip and oop asym str		3351	3346(4)	core ligand sym str
		3233(495)		$Ag^+(C_2H_2)_7$	3190	3192(637)	double-donor asym
	3315	3321(17), 3323(16)	ip and oop sym str		3205	3233(323)	str donor asym str
(4C) 332	3240/3272	3246(575)	3246(575) ip and oop asym str		3221	0-00 (0-0)	
		, ,			3262	3261(101), 3263	ext ligand asym str
	3326	3338(26)	ip and oop sym str		5-1-	(234)	
$Ag^{+}(C_2H_2)_5$ 3210	3210	3206(93)	oop donor asym str			3287(16)	oop double-donor
		3212(471)	ip donor asym str				sym str
	3239	3245(144)	core ligand asym str			3290(7)	ip double-donor sym
	3242	3252(133)	core ligand asym st			3334(11)	
	3262	3260(119)	ext ligand asym str	a		` '	donor sym str
	3311	3318(10)	oop donor sym str	"Calculated IR intensities (km/mol) are shown in parentheses; only bands with intensities >4 km/mol are listed. "ip" indicates in-phase			
	3328	3338(6)	core ligand sym str				
$Ag^+(C_2H_2)_5Ar$	3210	3207(92)	oop donor asym str	combination of two ligands; "oop" indicates out-of-phase combination of two ligands.			
		3213(471)	ip donor asym str				

shown in the Supporting Information, their infrared patterns do not agree with our experiments. Similar results were obtained previously for the coinage metal-acetylene complexes $Cu^+(C_2H_2)_n$ and $Au^+(C_2H_2)_n$ where all stable structures were found to be singlets. 49,50 We therefore exclude triplet states from further consideration here.

3239

3239(190)

core ligand asym str

To further investigate these silver-acetylene complexes, we measure the infrared spectra of size-selected ions by monitoring the fragmentation yield as a function of the infrared laser frequency. As shown above, the energy of an infrared photon in the C-H stretching region (3000-3500 cm⁻¹) is not enough to efficiently dissociate the smaller complexes. We employ rare-gas tagging to enhance the dissociation yields for these ions. 37,39,68-72 Upon photoexcitation in the C-H stretching region, $Ag^+(C_2H_2)_nAr$ complexes fragment by losing the argon atom. Tagging is known to sometimes produce isomers with different argon binding positions that have slightly different vibrational frequencies, and depending on the binding site, the frequencies may be somewhat different from those of the tag-free ion. We carefully investigate these effects with computations on both tagged and neat species. The spectra for the larger clusters were measured by the elimination of acetylene ligands for complexes larger than n = 4. The band positions measured for C-H stretches and the frequencies predicted by theory are presented in Table 3.

Figure 3 shows the infrared spectrum measured for $Ag^{+}(C_2H_2)Ar_2$. The spectra predicted by theory for the lowest

energy singlet-state Ag⁺(C₂H₂)Ar₂, Ag⁺(C₂H₂)Ar, and $Ag^{+}(C_2H_2)$ ions are also shown. Efficient fragmentation was not observed for $Ag^+(C_2H_2)Ar$ or the neat $Ag^+(C_2H_2)$ complex. This is not surprising because the computed binding energies (Table 2) are relatively high for these ions (31.71 and 6.85 kcal/mol, respectively). However, efficient elimination of argon was observed from the $Ag^{+}(C_{2}H_{2})Ar_{2}$ complex. This is expected because the energy of an IR photon in the C-H stretching region (~9 kcal/mol) is significantly greater than the calculated binding energy of argon in this complex (2.43 kcal/mol).

The $Ag^+(C_2H_2)Ar_2$ spectrum consists of two intense peaks at 3209 and 3296 cm⁻¹ and a weaker feature at 3227 cm⁻¹. All predicted spectra have two bands with frequency positions and relative intensities that are essentially identical with the experiment. This indicates that the argon atoms do not significantly affect the vibrations in this species. The minor band at 3227 cm⁻¹ is interesting. It could be explained by the presence of a positional isomer or ions in an unquenched excited triplet state. However, all Ag⁺(C₂H₂)Ar₂ isomers are predicted to have intense bands that are lower in frequency than the 3209 cm⁻¹ peak. Additionally, the triplet species is predicted to be 85.1 kcal/mol higher in energy than the ground state singlet, and its spectrum does not show any peaks near 3227 cm⁻¹. This is also the case for larger clusters. Another explanation for this band is that a Fermi resonance splits the asymmetric C-H stretch of the ground state $Ag^+(C_2H_2)Ar_2$ complex into two bands. It is well-known that acetylene has

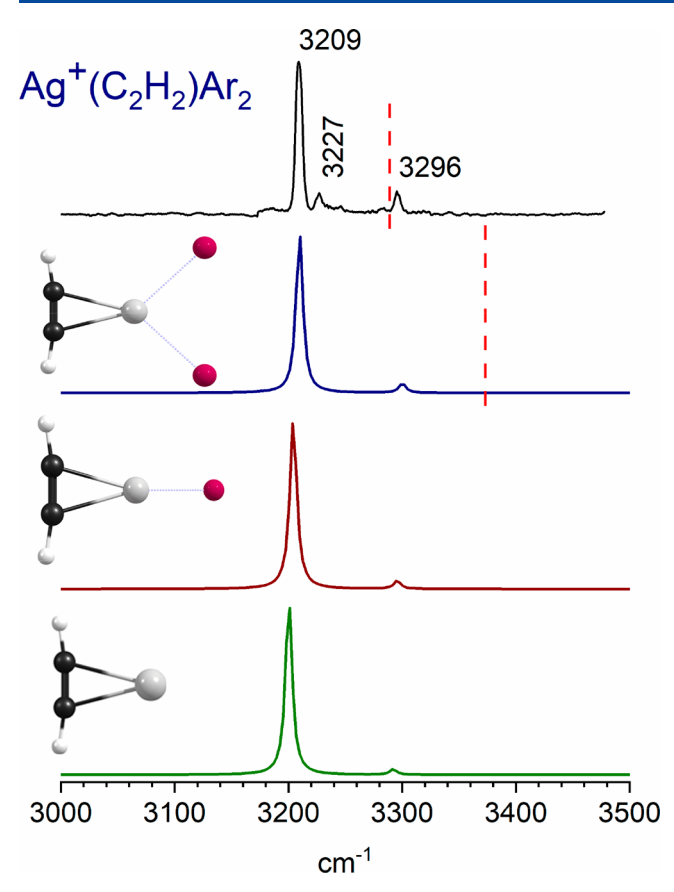


Figure 3. Infrared spectrum of $Ag^+(C_2H_2)Ar_2$ compared to the spectra predicted by DFT. The dashed vertical lines indicate the positions of the asymmetric and symmetric C–H stretches at 3289 and 3374 cm⁻¹, respectively.

such a Fermi resonance involving the overlap of the asymmetric C-H stretch with the $\nu_2 + \nu_4 + \nu_5$ combination band $(1974 + 612 + 730 \text{ cm}^{-1})$, which leads to a doublet with spacing of 13 cm⁻¹.62 The doublet spacing here is 18 cm⁻¹. Furthermore, the difference between the sum of computed frequencies for the combination band and the asymmetric C-H stretch in isolated acetylene is 27 cm⁻¹. The sum of the frequencies for these modes $(\nu_2 + \nu_4 + \nu_5)$ in the Ag⁺(C₂H₂)Ar₂ complex is computed to be 3246 cm⁻¹. This is only 37 cm⁻¹ higher than the asymmetric C-H stretch fundamental at 3209 cm⁻¹ and suggests that a Fermi resonance is feasible. We therefore tentatively assign the asymmetric stretch doublet as a Fermi resonance. If this assignment is correct, it is reasonable to expect the position of the minor feature to shift systematically in larger complexes as the frequency of the asymmetric C-H stretch changes.

The bands measured at 3209 and 3296 cm⁻¹ are red-shifted from the C–H vibrations in isolated acetylene. These positions are indicated by the dashed red lines at 3289 cm⁻¹ (asymmetric stretch) and 3374 cm⁻¹ (symmetric stretch).⁶² The symmetric stretch is not IR-active in free acetylene, but it is activated in these complexes because the hydrogen atoms bend away from the metal ion. Similar red-shifted frequencies have been previously reported for several metal cation—acetylene complexes. ^{46–50,52,53} The symmetric stretch measured here is red-shifted by 78 cm⁻¹ from this frequency in acetylene, while the two asymmetric stretch bands are 80 and 62 cm⁻¹ to the red. The recommended frequency for the

asymmetric stretch is 3289 cm⁻¹, but the Fermi doublet measured experimentally lies at 3295 and 3282 cm⁻¹.62 As explained above, in these metal cation- π systems, the metal ion withdraws bonding electron density from the HOMO of acetylene, which extends onto the CH bonds. The reduced bonding density results in weaker bonds and lower frequencies. Although the acetylene vibrational band shifts here are considerably smaller than they were for earlier transition metal ions (Ni⁺, Co⁺, Fe⁺, and V⁺), 48 they are consistent with the shifts observed for the coinage metals copper and gold as well as zinc. Evidently the acceptance of σ electron density and back-donation into the π^* orbitals of acetylene are less effective for these ions (Cu $^{\scriptscriptstyle +}$, Ag $^{\scriptscriptstyle +}$, Au $^{\scriptscriptstyle +}$, and Zn $^{\scriptscriptstyle +}$). This makes sense because of the filled d shells of these metal ions, which would inhibit the acceptance of σ electron density, and the high second ionization energies of the noble metals, which is consistent with less back-donation. The molecular orbitals of Ag+(acetylene) and the partial charges on the atoms in the complex compared to those of acetylene itself are shown in Figures S46 and S47. The positive charge of Ag⁺ is reduced to 0.91 in the complex, and that on the hydrogens increases as a result of the charge transfer.

The spectrum measured for $Ag^+(C_2H_2)_2Ar$ is shown in Figure 4 along with those predicted by theory for two

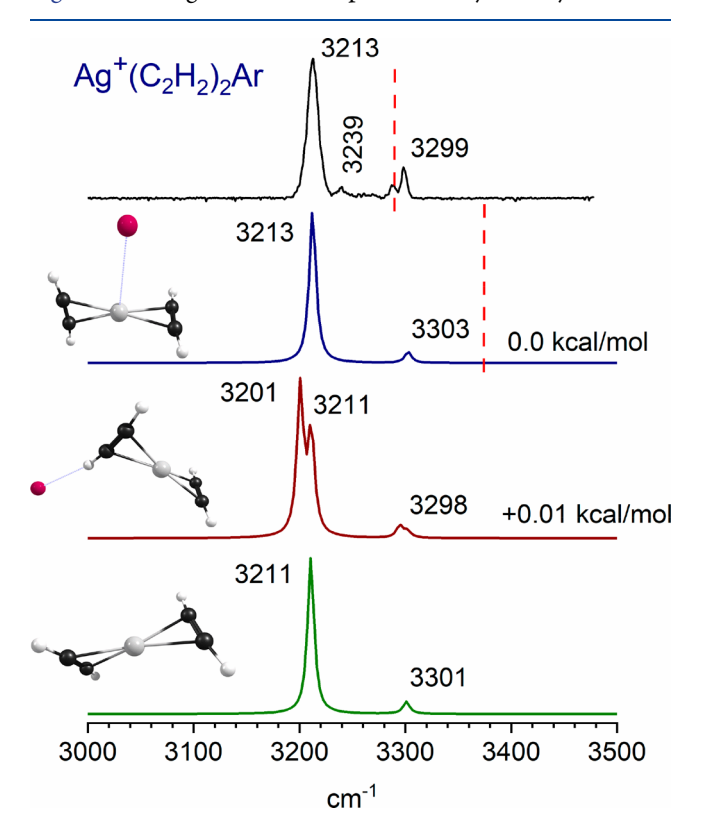


Figure 4. Infrared spectrum of $Ag^+(C_2H_2)_2Ar$ compared to the spectra predicted by DFT. The dashed vertical lines indicate the positions of the asymmetric and symmetric C–H stretches at 3289 and 3374 cm⁻¹, respectively.

 $Ag^+(C_2H_2)_2Ar$ isomers and $Ag^+(C_2H_2)_2$. The argon binding energy computed for this complex is 0.57 kcal/mol. This suggests that efficient photodissociation should occur upon absorption of a single photon in the C–H stretching region (photon energy, 8–10 kcal/mol). Indeed, we find that argon is eliminated efficiently, and two main bands are observed at

3213 and 3299 cm⁻¹. Theory shows that these correspond to the asymmetric and symmetric C–H stretches, respectively. Again, a minor feature is observed at a slightly higher frequency than the asymmetric C–H stretch band. Here, it appears at 3239 cm⁻¹, and a Fermi resonance is again a possible explanation for this band. Applying the same logic as above, the computed difference between the sum of the $\nu_2 + \nu_4 + \nu_5$ modes and the asymmetric C–H stretch fundamental is 45 cm⁻¹. The doublet spacing for this cluster size is 26 cm⁻¹. These values are slightly different from those reported for free acetylene (27 and 13 cm⁻¹, respectively). Nevertheless, given the uncertainty in the computed acetylene frequencies and the line widths in our spectra, the doublet can be assigned reasonably as originating from a Fermi resonance.

The C-H stretches here are also shifted to frequency lower than the values for acetylene. The positions of the free acetylene vibrations are indicated by dashed red lines and they reveal red-shifts for both the asymmetric and symmetric vibrations. These shifts are slightly less than those seen for the monoacetylene complex. This is consistent with a reduction in the ability of the Ag+ ion to exchange electron density with one ligand due to the presence of a second ligand. The predicted structure has two acetylene ligands forming η^2 cation— π bonds opposite each other in a D_{2d} arrangement. The spectra predicted for tagged and untagged ions are similar. However, as shown in the third trace, argon binding on the CH of one acetylene causes a slight splitting in both bands. This effect is less noticeable in the symmetric stretch when plotted at our resolution. Given the line widths in our spectra, it is likely that we are sampling both argon isomers. The n=2 species is therefore assigned as a structure with two π -bonded acetylene ligands coordinated to a silver ion with D_{2d} symmetry.

Figure 5 shows the spectrum for the $Ag^+(C_2H_2)_3Ar$ complex compared to those predicted by theory for two argon-tagged isomers and two tag-free isomers. As discussed above, this complex undergoes efficient dissociation via argon elimination. This is consistent with the low computed argon binding energy for this species (0.5 kcal/mol). A propeller-like structure with D_3 symmetry is calculated to be the ground state. A nearly isoenergetic isomer with C_2 symmetry is also predicted. Two nearly isoenergetic argon-tagged isomers are also found. As shown in the second and third traces, one isomer has a D_3 core with argon interacting with one ligand, while the other has argon interacting with two ligands to form a C_2 structure. These two isomers of the $Ag^+(C_2H_2)_3$ ion were previously reported by Krossing and co-workers in their study of salts containing this ion. 54 Their X-ray crystallography data revealed a structure with C_2 symmetry for the $Ag^+(C_2H_2)_3$, but theory predicted the D_3 structure to be the global minimum. Unfortunately, we cannot determine which isomer we have in our experiment because the spectra predicted for both isomers are identical and they match the experiment nearly perfectly. The spectral pattern for $Ag^+(C_2H_2)_3Ar$ is similar to that of the smaller complexes. An intense band at 3230 cm⁻¹ is assigned to the asymmetric C-H stretch, and a weaker band at 3315 cm⁻¹ is assigned to the symmetric C-H stretch. Yet again a minor feature that is not represented in the predicted spectra appears at higher frequency from the asymmetric C-H stretch band. Following the same logic used earlier, this band, shown here at 3252 cm⁻¹, is assigned to a Fermi resonance. Similar to the n = 1 and 2 species, the bands corresponding to the asymmetric and symmetric stretches are red-shifted. However, the shifts here are less relative to the vibrations of

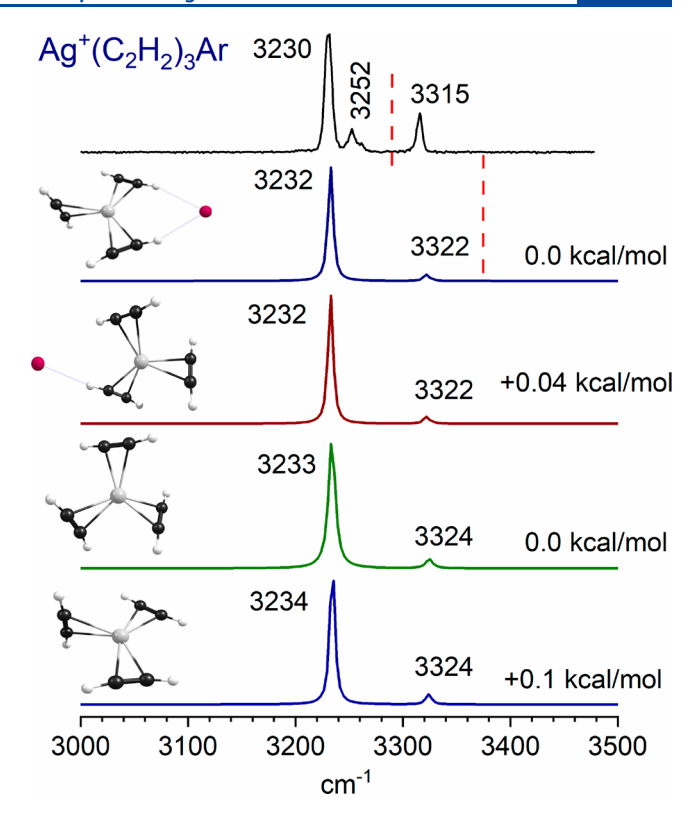


Figure 5. Infrared spectrum of $Ag^+(C_2H_2)_3Ar$ compared to the spectra predicted by DFT. The dashed vertical lines indicate the positions of the asymmetric and symmetric C–H stretches at 3289 and 3374 cm⁻¹, respectively.

free acetylene $(-59 \text{ and } -59 \text{ cm}^{-1})$ than those for the smaller complexes. Smaller shifts occur for complexes with additional ligands because the silver cation charge transfer is more delocalized. Again, tagging has a negligible effect on the spectrum, and there is excellent agreement between theory and experiment.

Figure 6 shows the spectrum for the $Ag^+(C_2H_2)_4$ complex, measured via argon elimination, compared to those predicted by theory for the tagged ion and the two low-lying 4C and 3C + 1 isomers. The computed binding energy for this complex shown in Table 2 (4.58 kcal/mol) suggests that IR photons in the C-H stretching region (8-10 kcal/mol) should cause fragmentation. Indeed, this species fragments via acetylene elimination; however, this process is not efficient, and the spectrum measured in this way is broad. Argon binds weakly to this complex (0.38 kcal/mol), and the tagged ion yields a higher quality spectrum. As shown in the figure, the spectra predicted for the tagged and tag-free species are almost identical. Theory finds that the most stable structure is a fourcoordinate (4C) species, although a three-coordinate species with one external ligand, indicated as "3C + 1", lies only slightly higher in energy. The spectrum predicted for the 3C + 1 ion does not match the measured spectrum, and it is unlikely that this species exists in our experiment. Once again, three features are observed with frequencies of 3240, 3272, and 3326 ${\rm cm}^{-1}$. The two main bands at 3240 and 3326 ${\rm cm}^{-1}$ correspond to the asymmetric and symmetric C-H stretches, and the weaker one at 3272 cm⁻¹ is assigned to the same Fermi resonance as in the smaller complexes. As seen previously, these bands are also red-shifted from the free acetylene vibrations. However, compared to smaller complexes, these

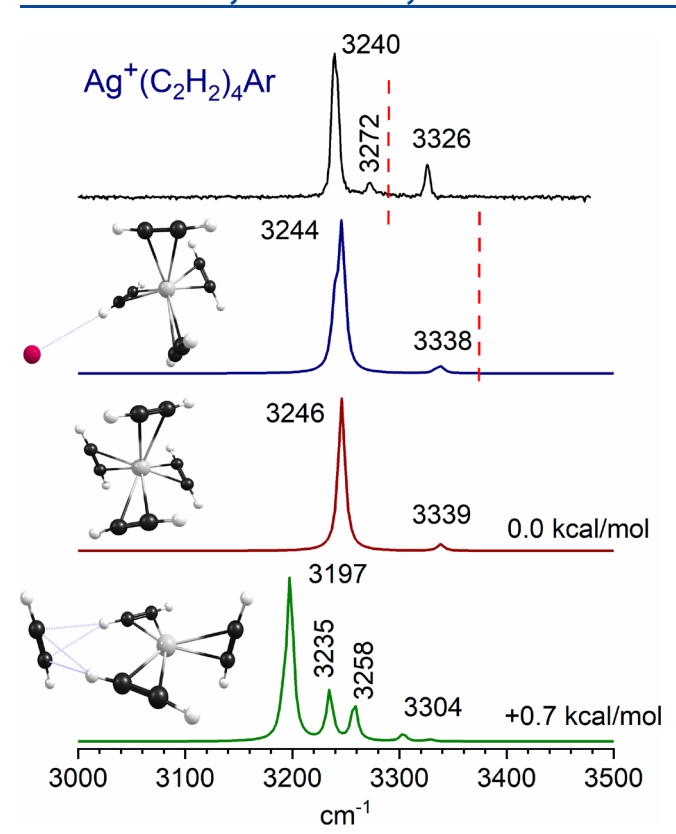


Figure 6. Infrared spectrum of $Ag^+(C_2H_2)_4$ compared to the spectra predicted by DFT for the 4C tetrahedral and 3C + 1 isomers.

shifts are smaller again $(-49 \text{ and } -48 \text{ cm}^{-1})$ due to the greater charge delocalization. There is excellent agreement between the measured and predicted spectra. Therefore, the n=4 complex is a near-tetrahedral species with Ag^+ interacting with four ligands via equivalent η^2 bonds. A similar 4C structure for the $Ag^+(C_2H_2)_4$ complex was reported by Krossing and coworkers using X-ray diffraction of ions in a salt crystal. S4

Figure 7 shows the spectrum of the $Ag^+(C_2H_2)_5$ and Ag+(C2H2)sAr ions measured via acetylene or argon elimination, respectively. Based on fragmentation data and computed binding energies, both fragmentation channels are expected to be efficient. However, the tagged spectrum is noticeably sharper and better resolved than the tag-free spectrum. This is understandable because the lower binding energies of these ions (0.29 kcal/mol for $Ag^+(C_2H_2)_5Ar$ vs 3.25 kcal/mol for $Ag^+(C_2H_2)_5$) allow single-photon dissociation. The spectrum for the tag-free ion may be biased toward somewhat hotter molecules, whose internal energy facilitates the dissociation. Because of this, the tagged complex is expected to give the most accurate representation of the n = 5spectrum. It is anticipated that the addition of an external ligand to the $Ag^+(C_2H_2)_4$ core ion would yield a spectrum that preserves the n = 4 bands and has new features corresponding to the external ligand that are weaker than those of the core ion. However, the spectrum is surprisingly different from that of the n = 4 complex, with six bands in the C-H stretching region (3210, 3239, 3246, 3262, 3310, and 3326 cm⁻¹). There is a 30 cm⁻¹ difference between the most intense features in the $Ag^+(C_2H_2)_4$ and $Ag^+(C_2H_2)_5$ spectra. Clearly the solvating ligand is not a passive addition but actively alters the IR resonances of the core ion. Fortunately, theory can help interpret these intriguing patterns.

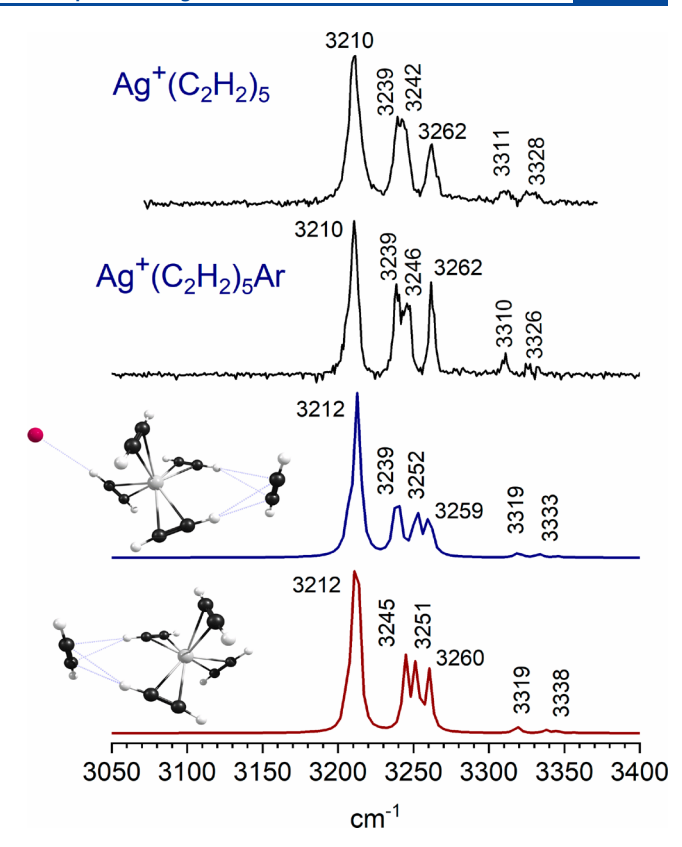


Figure 7. Infrared spectrum of $Ag^+(C_2H_2)_5$ and $Ag^+(C_2H_2)_5Ar$ compared to the spectra predicted by DFT.

According to theory, the bands seen here at 3239/3246 cm⁻¹ and at 3326 cm⁻¹ correspond to the same kind of vibrations seen for the $Ag^{+}(C_2H_2)_4$ core ion at 3240 and 3326 cm⁻¹. These features are assigned as the asymmetric and symmetric C-H vibrations of the core ligands that are not interacting with the external ligand. A slight splitting in the asymmetric stretch band is observed because the external ligand lowers the symmetry of the molecule and the core ligands are no longer equivalent. The other three bands result from vibrations involving the external ligand. The most intense feature at 3210 cm⁻¹ results from the in-phase and out-ofphase asymmetric vibrations of two core ligands donating CH groups into the π system of the external ligand. Ligands involved in this type of $CH-\pi$ hydrogen bond have strongly red-shifted vibrations with enhanced intensity. Similar behavior was observed previously for the copper and gold cation—acetylene complexes. 49,50 The band at 3310 cm⁻¹ is assigned to the in-phase and out-of-phase symmetric stretches of these same ligands. Finally, the feature at 3262 cm⁻¹ is the asymmetric stretch of the external ligand. This band is slightly red-shifted from the asymmetric stretch of free acetylene at 3289 cm⁻¹ due to polarization of acetylene by the silver cation. Interestingly, the vibration of this external ligand was found in almost the same place at 3263 cm⁻¹ for both Cu⁺(C₂H₂)₅ and Au⁺(C₂H₂)₅. As expected, the symmetric stretches of these ligands have little or no intensity, and most are not detected. However, the bands at 3310 and 3326 cm⁻¹ correspond to the symmetric stretches of the single donor and core ligands, respectively. As seen for the previously studied copper and gold cation-acetylene complexes, the solvating acetylene ligands here also form $CH-\pi$ hydrogen bonds which

significantly perturb the C–H vibrations of the donor ligands in the core ion.

Figure 8 shows the spectrum measured for the $Au^+(C_2H_2)_6$ complex via acetylene elimination. Surprisingly, the pattern

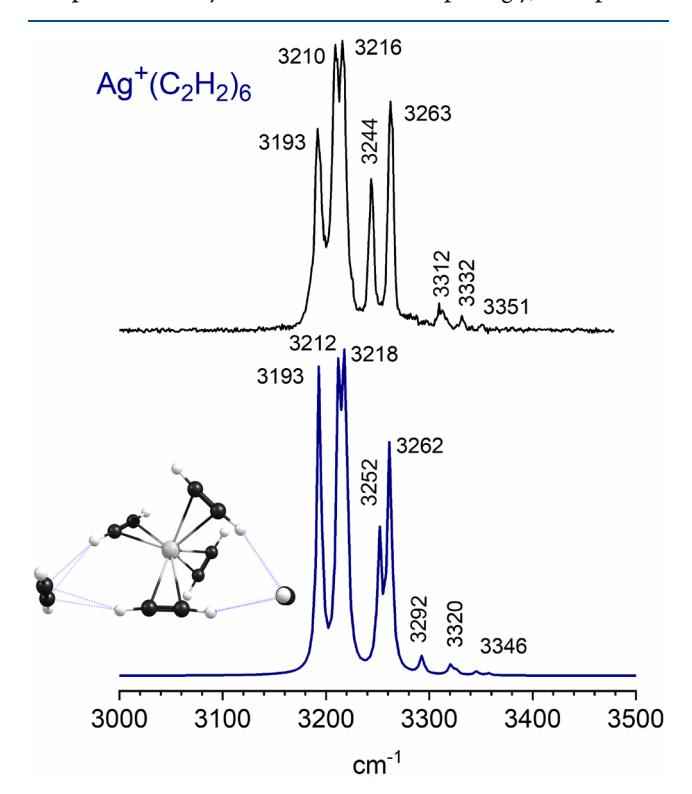


Figure 8. Infrared spectrum of $Ag^+(C_2H_2)_6$ compared to the spectrum predicted by DFT.

here is more complicated than that of the n = 5 complex, with eight IR bands detected. Again, we turn to theory to interpret this spectrum. The predicted structure has a four-ligand core with two external ligands interacting with three core ligands via bifurcated $CH-\pi$ hydrogen bonds. This results in one core double-donor ligand that interacts with both external ligands, two single donors, and a core ligand that does not interact with an external ligand. The band at 3244 cm⁻¹ corresponds to the asymmetric vibration of the core ligand that is not solvated. The same vibration was observed as the 3239/3246 cm⁻¹ doublet in Ag⁺(C₂H₂)₅ and the intense 3240 cm⁻¹ band for the $Ag^{+}(C_2H_2)_4$ core ion. The remaining bands are from vibrations involving $CH-\pi$ hydrogen bonds, and yet again, they have enhanced intensities and are the most red-shifted. The vibration observed and predicted at 3193 cm⁻¹ is the asymmetric stretch of the unique double-donor core ligand, which forms hydrogen bonds with two external ligands. This ligand is the most highly solvated and its vibration is shifted farthest to the red. The bands at 3210 and 3216 cm⁻¹ are analogous to the 3210 cm⁻¹ feature for the n = 5 complex, corresponding to the in-phase and out-of-phase asymmetric stretches of a single-donor ligand. However, the splitting observed here is due to the two inequivalent single-donor ligands in the n = 6 complex. Similarly, the 3263 cm⁻¹ band seen here corresponds to the 3262 cm⁻¹ band first observed for the n = 5 complex. However, in this case, the band results from the asymmetric stretches of two external ligands. Except for the double-donor band at 3193 cm⁻¹, the asymmetric vibrations of the n = 6 complex produce bands that correspond to similar ones for the n = 5 species. The symmetric vibrations are characteristically weak, and the bands at 3312, 3332, and 3351 cm⁻¹ are assigned to the symmetric stretches of the double-donor, single-donor, and core ligands, respectively.

The experimental spectrum and three simulated spectra for the $Ag^+(C_2H_2)_7$ complex are shown in Figure 9. Multiple

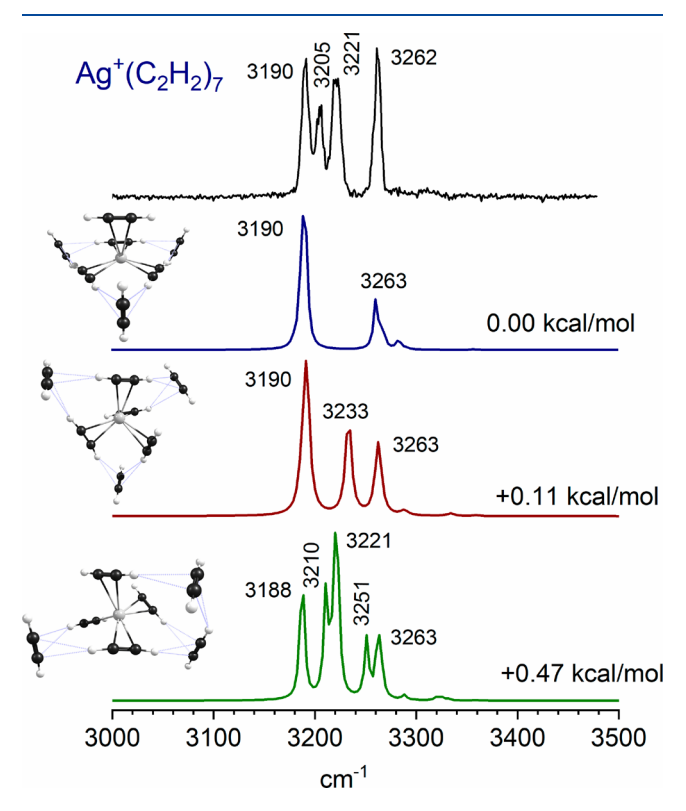


Figure 9. Infrared spectrum of $Ag^+(C_2H_2)_7$ compared to the spectra predicted by DFT.

isomers with comparable energies (within 0.47 kcal/mol) were identified by theory for this complex, differing only in the position and orientation of the ligands that solvate the n = 4core. All simulated spectra reproduce the intense 3190 and 3262 cm⁻¹ bands which correspond to the double-donor asymmetric stretch and the external asymmetric stretch, respectively. This is not surprising because the predicted structures all show three acetylene molecules solvating the $Ag^{+}(C_2H_2)_4$ ion by forming $CH-\pi$ hydrogen bonds. The multiple double-donor ligands and three external ligands produce the characteristic strongly red-shifted band at 3190 cm⁻¹ and the intense feature at 3262 cm⁻¹, respectively. The band corresponding to the asymmetric vibration of a core ligand, previously seen at 3244 cm⁻¹, is not detected here, indicating that all the core ligands are solvated. Accordingly, the predicted spectra only differ from each other and the measured spectrum in the position of the bands corresponding to core single-donor ligands. The structure in the fourth trace of the figure has bands at 3210 and 3221 cm⁻¹ that are consistent with those measured at 3205 and 3221 cm⁻¹. Because of their similar energetics and predicted spectra matching the main experimental bands for the n = 7 complex, it is possible that all three isomers are present in our experiment. Another possibility to consider is that the acetylene ligands undergo an intracluster reaction to form benzene. This type of behavior was recently reported for

vanadium cation-acetylene complexes. 52 The spectrum predicted for such a reacted Ag⁺(C₆H₆)₂(C₂H₂) complex is presented in the Supporting Information. It does not match the measured $Ag^+(C_2H_2)_7$ spectrum, indicating that such a reaction does not occur here. This is not surprising because there is usually a significant activation barrier to form benzene in metal-acetylene species. Accordingly, it is most likely that our spectrum just represents multiple isomers with solvating acetylenes in different positions.

We have also measured spectra for the Ag+(C2H2)8 and Ag⁺(C₂H₂)₉ complexes, which are shown in the Supporting Information. These larger complexes have the same two main bands seen for the n = 7 complex at 3190 and 3262 cm⁻¹ but with greater line widths. Theory also predicts several structures with similar relative energies for each of these ions that vary in the position and orientation of the external ligands around the n = 4 core. Apparently, we do not produce any specific structure for these larger complexes but sample an assortment of solvated n = 4 structures. The evolution of the spectral patterns with increasing cluster size is quite compelling. This is presented in Figure 10 for the n = 4-7 species along with the associated vibrational bands for different types of ligands (core, single donor, double donor, and external).

It is interesting to compare the coordination behavior found here for the silver-acetylene system to those previously reported for the corresponding complexes of copper and gold. 49,50 As established above, η^2 metal cation—acetylene bonding configurations are expected for each of these

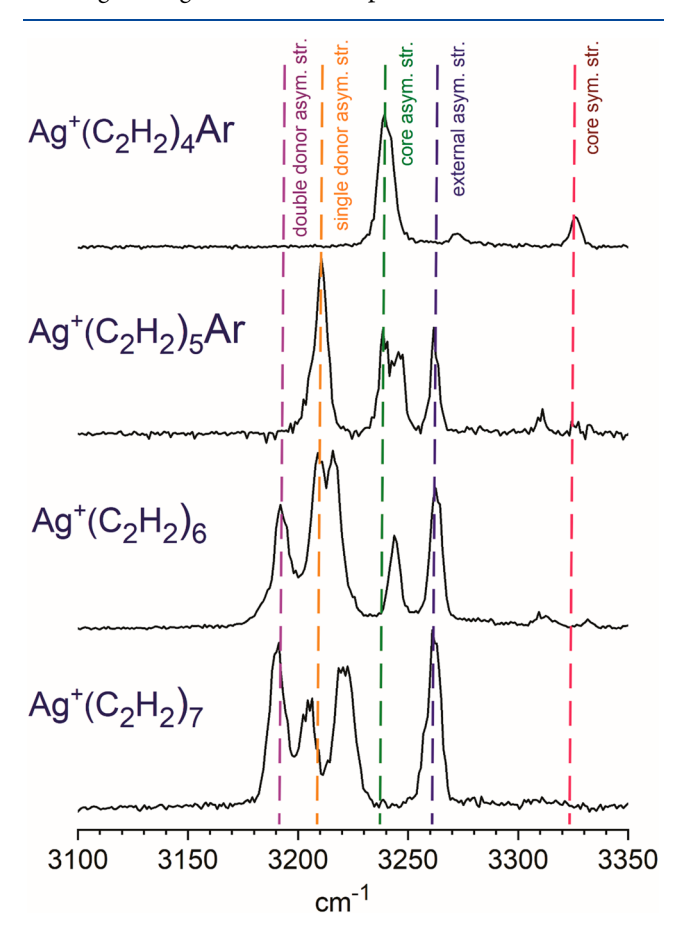


Figure 10. Comparison of the spectra for the $Ag^{+}(C_2H_2)_{4-7}$ complexes, demonstrating the evolution of different vibrational features as the solvation sphere develops.

complexes. However, their coordination behavior is less predictable. Figure 11 shows the infrared spectra for the

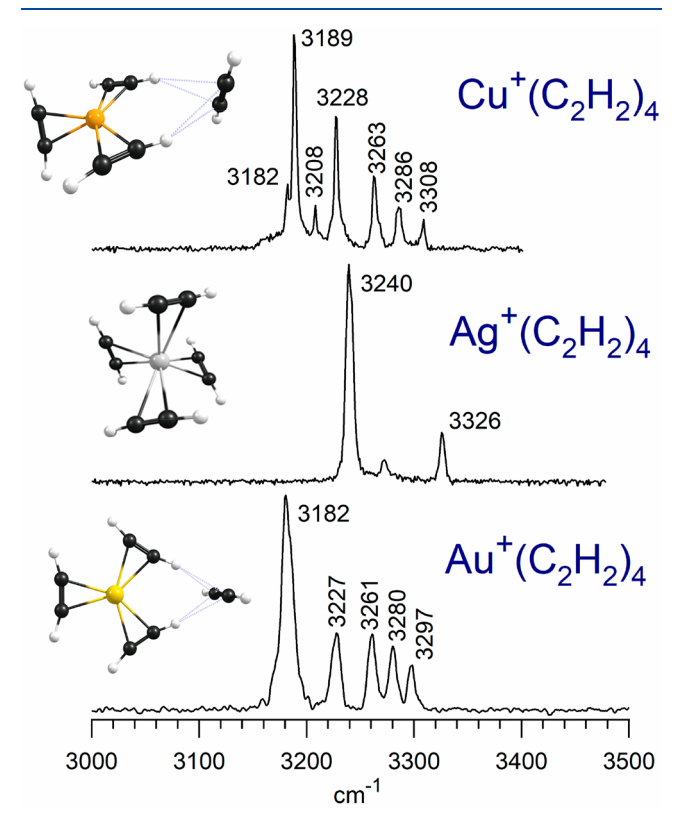


Figure 11. Comparison of the spectra for the $M^+(C_2H_2)_4$ complexes for the coinage metals (Cu, Ag, and Au).

 $M^+(C_2H_2)_4$ complexes of copper, silver, and gold. The $Ag^{+}(C_{2}H_{2})_{4}$ species has a tetrahedral four-coordinate (4C) structure, whereas the $Cu^+(C_2H_2)_4$ and $Au^+(C_2H_2)_4$ ions have a 3C + 1 structure. Corresponding to this, the spectrum for silver is noticeably different from the others. The only other four-coordinate cation-acetylene complexes we have found are those for Ni⁺(C₂H₂)₄ complexes.⁴⁷ The variation in coordination number for different coinage metal ion-ligand complexes has been investigated previously. 73-75 Di-, tri-, and tetracoordinate structures are well documented for coinage metal-ligand systems. However, predicting the coordination number for a specific metal-ligand combination is challenging.⁷⁵ Higher coordination numbers for silver have also been reported in gas-phase studies. 73,74 Jiang and co-workers reported that copper cation-CO₂ complexes have a coordination number of six, while silver-CO₂ complexes are coordinated to eight ligands.⁷³ In a study of singly charged metal cation-methane complexes, Metz and co-workers reported that the copper cation binds to four ligands, whereas silver binds six. 74 Therefore, the tetracoordinate silveracetylene complex observed here is consistent with previously reported trends. Additionally, it is well-known that the atomic radius of gold is anomalously lower than that of silver because of relativistic effects. The computed M-C bond distances for M⁺(C₂H₄) complexes of copper, silver, and gold were shown to increase in the order Cu < Au < Ag by Hartwig et al.³² Indeed, we see a similar trend in the M-C bond distances for $M^{+}(C_2H_2)$ complexes (Cu-2.09 Å < Au-2.22 Å < Ag-2.36 Å). It is therefore understandable that the larger silver cation can accommodate an additional ligand in its coordination sphere.

The nonspecific binding of solvating acetylene molecules in this system is somewhat surprising. Previous studies on copper- and gold-acetylene ions showed that larger complexes consisted of a 3C core with three equivalent cavity-like binding sites that could accommodate one solvating ligand each. The result was a $M^+(C_2H_2)_6$ complex (M = Cu and Au) with a secondary solvent shell defining an appealing D_{3h} structure. The stability of this secondary solvation shell was great enough to distort the 3C core acetylene structure from a propeller to a planar configuration, which could better accommodate the solvating ligands. In the present case, although the n = 4 acetylene binding is rather low, no such solvent-induced rearrangement occurs. The nearly tetrahedral 4C core ion is apparently stable enough to retain its structure, but this precludes the symmetric organization of second-sphere ligand/solvent molecules seen for copper and gold. The larger silver cation also forms longer M-C bonds with weaker metal cation-acetylene interactions. Correspondingly, the computed binding energies for acetylene in M⁺(C₂H₂) complexes are 42.6, 31.7, and 53.3 kcal/mol for copper, silver, and gold, respectively. This weaker binding for silver cation is also reflected in the relatively small red-shifts observed for the acetylene vibrations here compared to those of other metalacetylene complexes. Finally, it is likely that the relatively weak silver-acetylene binding permits the observation of the Fermi resonance known for isolated acetylene. It will be interesting to investigate other weakly bound metal cation-acetylene species to see whether this pattern persists.

CONCLUSION

Silver-acetylene cations of the form $Ag^{+}(C_2H_2)_n$ $(n = 1-9)_n$ and their argon-tagged analogues, Ag+(C2H2),Arm, were produced and studied with mass-selected infrared photodissociation spectroscopy in the C-H stretching region. The structures and coordination numbers of these complexes are determined by examining their fragmentation patterns and distinctive spectra and comparing them to the predictions of theory. All Ag⁺(C₂H₂)_n complexes were found to have d¹⁰ singlet ground state configurations. Smaller complexes (n = 1 -4) have IR-active bands that are shifted to lower frequencies than the C-H vibrations in acetylene. The red shifts observed for unsaturated complexes in this study are the smallest seen yet for transition metal ion-acetylene systems. This is likely due to weak silver ion-acetylene binding resulting from an inability of the filled d10 orbitals in silver to accept or donate electron density efficiently. The four-coordinate (4C) $Ag^{+}(C_{2}H_{2})_{4}$ complex is the fully coordinated species. The near-tetrahedral structure of this core ion produces multiple binding sites where additional acetylene ligands can bind, leading to multiple isomers for larger complexes. This nonspecific binding produces isomers that are energetically similar and only differ in the position and orientation of the solvating ligands. Nevertheless, specific vibrational signatures identify each type of ligand as core, single donor, double donor, or external. The silver-acetylene system provides yet another fascinating example of cation- π and CH- π hydrogen bonding.

ASSOCIATED CONTENT

Supporting Information

The Supporting Information is available free of charge at https://pubs.acs.org/doi/10.1021/acs.jpca.0c08081.

Full details of the DFT computations done in support of the spectroscopy presented here, including the structures, energetics, and vibrational frequencies for each of the complexes considered, and the predicted spectra for singlet versus triplet electronic states; full citation for ref 60 (PDF)

AUTHOR INFORMATION

Corresponding Author

Michael A. Duncan — Department of Chemistry, University of Georgia, Athens, Georgia 30602, United States; ocid.org/0000-0003-4836-106X; Email: maduncan@uga.edu

Authors

Antonio D. Brathwaite – Department of Chemistry, Emory University, Atlanta, Georgia 30322, United States

Timothy B. Ward – Department of Chemistry, University of Georgia, Athens, Georgia 30602, United States

Joshua H. Marks – Department of Chemistry, University of Georgia, Athens, Georgia 30602, United States

Complete contact information is available at: https://pubs.acs.org/10.1021/acs.jpca.0c08081

Note:

The authors declare no competing financial interest.

ACKNOWLEDGMENTS

We acknowledge generous support for this work from the U.S. Department of Energy, Office of Science, Basic Energy Sciences, Division of Chemical, Geological, and Biosciences (Grant DE-SC0018835) and the National Science Foundation through Grant CHE-1764111.

REFERENCES

- (1) Huheey, J. E.; Keiter, E. A.; Keiter, R. L. Inorganic Chemistry Principles of Structure and Reactivity; Harper Collins: New York, 1993.
- (2) Freiser, B. S., Ed.; Organometallic Ion Chemistry; Kluwer: Dordrecht, The Netherlands, 1996.
- (3) Nakamoto, K. Infrared and Raman Spectra of Inorganic and Coordinated Compounds, 5th ed.; Wiley: New York, 1997.
- (4) Cotton, F. A. Advanced Inorganic Chemistry, 6th ed.; John Wiley and Sons, Inc.: New York, 1999.
- (5) Crabtree, R. H. The Organometallic Chemistry of the Transition Metals, 5th ed.; John Wiley & Sons: Hoboken, NJ, 2009.
- (6) Hartwig, J. F. Organotransition Metal Chemistry; University Science Books: Sausalito, CA, 2010.
- (7) Bertini, I.; Gray, H. B.; Stiefel, E. I.; Valentine, J. S. *Biological Inorganic Chemistry: Structure and Reactivity*; University Science Books: Sausalito, CA, 2007.
- (8) Steed, J. W.; Atwood, J. L. Supramolecular Chemistry; John Wiley & Sons: Chichester, UK, 2009.
- (9) Dougherty, D. A. Cation- π Interactions in Chemistry and Biology: A New View of Benzene, Phe, Tyr, and Trp. Science 1996, 271, 163–168.
- (10) Ma, J. C.; Dougherty, D. A. The Cation- π Interaction. *Chem. Rev.* **1997**, *97*, 1303–1324.
- (11) Trotuş, I.-T.; Zimmermann, T.; Schüth, F. Catalytic Reactions of Acetylene: A Feedstock for the Chemical Industry Revisited. *Chem. Rev.* **2014**, *114*, 1761–1782.

- (12) Kennedy, C. R.; Lin, S.; Jacobsen, E. N. The Cation- π Interaction in Small-Molecule Catalysis. *Angew. Chem., Int. Ed.* **2016**, 55, 12596–12624.
- (13) Neel, A. J.; Hilton, M. J.; Sigman, M. S.; Toste, F. D. Exploiting Non-Covalent Cation- π Interactions for Catalyst Design. *Nature* **2017**, 543, 637–646.
- (14) Davis, M. E. New Vistas in Zeolite and Molecular Sieve Catalysis. Acc. Chem. Res. 1993, 26, 111–115.
- (15) Broclawik, E.; Załucka, J.; Kozyra, P.; Mitoraj, M.; Datka, J. New Insights into Charge Flow Processes and their Impact on the Activation of Ethene and Ethyne by Cu(I) and Ag(I) Sites in MFI. J. Phys. Chem. C 2010, 114, 9808–9816.
- (16) Lee, J. Y.; Farha, O. K.; Roberts, J.; Scheidt, K. A.; Nguyen, S. T.; Hupp, J. T. Metal-Organic Framework Materials as Catalysts. *Chem. Soc. Rev.* **2009**, *38*, 1450–1459.
- (17) Xiang, S.; Zhou, W.; Gallegos, J. M.; Liu, Y.; Chen, B. Exceptionally High Acetylene Uptake in a Microporous Metal-Organic Framework with Open Metal Sites. *J. Am. Chem. Soc.* **2009**, *131*, 12415–12419.
- (18) Moreau, F.; da Silva, I.; Al Smail, N. H.; Easun, T. L.; Savage, M.; Godfrey, H. G. W.; Parker, S. F.; Manuel, P.; Yang, S.; Schröder, M. Unravelling Exceptional Acetylene and Carbon Dioxide Adsorption within a Tetra-Amide Functionalized Metal-Organic Framework. *Nat. Commun.* 2017, *8*, 14085.
- (19) Eller, K.; Schwarz, H. Organometallic Chemistry in the Gas Phase. Chem. Rev. 1991, 91, 1121–1171.
- (20) Gibson, J. K. Gas-Phase Reactions of Tc⁺, Re⁺, Mo⁺ and Cu⁺ with Alkenes. *J. Organomet. Chem.* **1998**, 558, 51–60.
- (21) Willey, K. F.; Cheng, P. Y.; Bishop, M. B.; Duncan, M. A. Charge-Transfer Photochemistry in Ion-Molecule Cluster Complexes of Silver. *J. Am. Chem. Soc.* **1991**, *113*, 4721–4728.
- (22) Sharma, P.; Attah, I.; Momoh, P.; El-Shall, M. S. Metal Acetylene Cluster Ions $M^+(C_2H_2)_n$ as a Model for Studying Reactivity of Laser-Generated Transition Metal Cations. *Int. J. Mass Spectrom.* **2011**, 300, 81–90.
- (23) Gidden, J.; Van Koppen, P. A. M.; Bowers, M. T. Dehydrogenation of Ethene by Ti⁺ and V⁺: Excited State Effects on the Mechanism for C–H Bond Activation from Kinetic Energy Release Distributions. *J. Am. Chem. Soc.* **1997**, *119*, 3935–3941.
- (24) Manard, M. J.; Kemper, P. R.; Bowers, M. T. Binding Interactions of Mono- and Diatomic Silver Cations with Small Alkenes: Experiment and Theory. *Int. J. Mass Spectrom.* **2005**, *241*, 109–117.
- (25) Manard, M. J.; Kemper, P. R.; Carpenter, C. J.; Bowers, M. T. Dissociation Reactions of Diatomic Silver Cations with Small Alkenes: Experiment and Theory. *Int. J. Mass Spectrom.* **2005**, 241, 99–108.
- (26) Dunbar, R. C. Photodissociation of Trapped Ions. Int. J. Mass Spectrom. 2000, 200, 571-589.
- (27) Sievers, M. R.; Jarvis, L. M.; Armentrout, P. B. Transition Metal Ethene Bonds: Thermochemistry of $M^+(C_2H_4)_n$ (M=Ti-Cu, n=1 and 2) Complexes. *J. Am. Chem. Soc.* **1998**, *120*, 1891–1899.
- (28) Fisher, E. R.; Armentrout, P. B. Reactions of Co⁺, Ni⁺, and Cu⁺ with Cyclopropane and Ethylene Oxide. Metal-Methylidene Ion Bond Energies. *J. Phys. Chem.* **1990**, *94*, 1674–1683.
- (29) Operti, L.; Rabezzana, R. Gas Phase Ion Chemistry in Organometallic Systems. *Mass Spectrom. Rev.* **2006**, 25, 483–513.
- (30) Sodupe, M.; Bauschlicher, C. W., Jr. Theoretical Study of the Bonding of the First- and Second-Row Transition-Metal Positive Ions to Acetylene. *J. Phys. Chem.* **1991**, *95*, 8640–8640.
- (31) Sodupe, M.; Bauschlicher, C. W., Jr.; Langhoff, S. R.; Partridge, H. Theoretical Study of the Bonding of the First-Row Transition-Metal Positive Ions to Ethylene. *J. Phys. Chem.* **1992**, *96*, 2118–2122.
- (32) Hertwig, R. H.; Koch, W.; Schröder, D.; Schwarz, H.; Hrušák, J.; Schwerdtfeger, P. A Comparative Computational Study of Cationic Coinage Metal-Ethylene Complexes $(C_2H_4)M^+$ (M = Cu, Ag, and Au). J. Phys. Chem. 1996, 100, 12253–12260.
- (33) Stockigt, D.; Schwarz, J.; Schwarz, H. Theoretical and Experimental Studies on the Bond Dissociation Energies of

- Al(methane)⁺, Al(acetylene)⁺, Al(ethene)⁺, and Al(ethane)⁺. J. Phys. Chem. **1996**, 100, 8786–8790.
- (34) Frenking, G.; Fröhlich, N. The Nature of the Bonding in Transition Metal Compounds. *Chem. Rev.* **2000**, *100*, 717–774.
- (35) Klippenstein, S. J.; Yang, C.-N. Density Functional Theory Predictions for the Binding of Transition Metal Cations to Pi Systems: From Acetylene to Coronene and Tribenzocyclyne. *Int. J. Mass Spectrom.* **2000**, 201, 253–267.
- (36) Wesolowski, S. S.; King, R. A.; Schaefer, H. F.; Duncan, M. A. Coupled-Cluster Electronic Spectra for the Ca⁺-Acetylene π Complex and Comparisons to its Alkaline Earth Analogs. *J. Chem. Phys.* **2000**, 113, 701–706.
- (37) Duncan, M. A. Spectroscopy of Metal Ion Complexes: Gas Phase Models for Solvation. *Annu. Rev. Phys. Chem.* **1997**, 48, 69–93.
- (38) Duncan, M. A. Frontiers in the Spectroscopy of Mass-Selected Molecular Ions. *Int. J. Mass Spectrom.* **2000**, 200, 545–569.
- (39) Baer, T.; Dunbar, R. C. Ion Spectroscopy: Where Did It Come From; Where Is It Now; and Where Is It Going? *J. Am. Soc. Mass Spectrom.* **2010**, *21*, 681–693.
- (40) France, M. R.; Pullins, S. H.; Duncan, M. A. Spectroscopy of the Ca⁺-Acetylene π Complex. *J. Chem. Phys.* **1998**, *108*, 7049–7051.
- (41) Reddic, J. E.; Duncan, M. A. Photodissociation Spectroscopy $Mg^+-C_2H_2$ π Complex. Chem. Phys. Lett. **1999**, 312, 96–100.
- (42) Chen, J.; Wong, T. H.; Cheng, Y. C.; Montgomery, K.; Kleiber, P. D. Photodissociation Spectroscopy and Dynamics of MgC₂H₄⁺. *J. Chem. Phys.* **1998**, *108*, 2285–2293.
- (43) Chen, J.; Wong, T.-H.; Kleiber, P. D.; Yang, K.-H. Photofragmentation Spectroscopy of Al⁺(C₂H₄). *J. Chem. Phys.* **1999**, 110, 11798–11805.
- (44) Lu, W.-Y.; Liu, R.-G.; Wong, T.-H.; Chen, J.; Kleiber, P. D. Photoinduced Charge Transfer Dissociation of Al⁺-Ethene, -Propene and Butene. *J. Phys. Chem. A* **2002**, *106*, 725–730.
- (45) Stringer, K. L.; Citir, M.; Metz, R. B. Photofragment Spectroscopy of π Complexes: Au⁺(C₂H₄) and Pt⁺(C₂H₄). *J. Phys. Chem. A* **2004**, *108*, 6996–7002.
- (46) Walters, R. S.; Jaeger, T. D.; Duncan, M. A. Infrared Spectroscopy of $Ni^+(C_2H_2)_n$ Complexes: Evidence for Intracluster Cyclization Reactions. *J. Phys. Chem. A* **2002**, *106*, 10482–10487.
- (47) Walters, R. S.; Pillai, E. D.; Schleyer, P. v. R.; Duncan, M. A. Vibrational Spectroscopy and Structures of $\mathrm{Ni}^+(C_2H_2)_n$ (n = 1–4) Complexes. *J. Am. Chem. Soc.* **2005**, *127*, 17030–17042.
- (48) Walters, R. S.; Schleyer, P. v. R.; Corminboeuf, C.; Duncan, M. A. Structural Trends in Transition Metal Cation-Acetylene Complexes Revealed through the C–H Stretching Fundamentals. *J. Am. Chem. Soc.* **2005**, *127*, 1100–1101.
- (49) Brathwaite, A. D.; Ward, T. B.; Walters, R. S.; Duncan, M. A. Cation-π and CH-π Interactions in the Coordination and Solvation of Cu⁺(Acetylene)_n Complexes. *J. Phys. Chem. A* **2015**, *119*, 5658–5667.
- (50) Ward, T. B.; Brathwaite, A. D.; Duncan, M. A. Infrared Spectroscopy of Au(Acetylene)_n⁺ Complexes in the Gas Phase. *Top. Catal.* **2018**, *61*, 49–61.
- (51) Marks, J. H.; Ward, T. B.; Duncan, M. A. Infrared Spectroscopy of the Coordination and Solvation in $Cu^+(C_2H_4)_n$ (n = 1–9) Complexes. *Int. J. Mass Spectrom.* **2019**, 435, 107–113.
- (52) Marks, J. H.; Ward, T. B.; Brathwaite, A. D.; Ferguson, S.; Duncan, M. A. Cyclotrimerization of Acetylene in Gas Phase $V^+(C_2H_2)_n$ Complexes: Detection of Intermediates and Products with Infrared Spectroscopy. *J. Phys. Chem. A* **2019**, *123*, 6733–6743.
- (53) Marks, J. H.; Ward, T. B.; Brathwaite, A. D.; Duncan, M. A. Infrared Spectroscopy of Zn(Acetylene)_n⁺ Complexes: Ligand Activation and Nascent Polymerization. *J. Phys. Chem. A* **2020**, *124*, 4764–4776.
- (54) Reisinger, A.; Trapp, N.; Krossing, I.; Altmannshofer, S.; Herz, V.; Presnitz, M.; Scherer, W. Homoleptic Silver(I) Acetylene Complexes. *Angew. Chem., Int. Ed.* **2007**, *46*, 8295–8298.
- (55) Duncan, M. A. Laser Vaporization Cluster Sources. Rev. Sci. Instrum. 2012, 83, 041101.
- (56) LaiHing, K.; Taylor, T. G.; Cheng, P. Y.; Willey, K. F.; Peschke, M.; Duncan, M. A. Photodissociation in a Reflectron Time-of-Flight

- Mass Spectrometer: A Novel MS/MS Scheme for High Mass Systems. *Anal. Chem.* **1989**, *61*, 1458–1460.
- (57) Cornett, D. S.; Peschke, M.; LaiHing, K.; Cheng, P. Y.; Willey, K. F.; Duncan, M. A. Reflectron Time-of-Flight Mass Spectrometer for Laser Photodissociation. *Rev. Sci. Instrum.* **1992**, *63*, 2177–2186.
- (58) Duncan, M. A. Infrared Spectroscopy to Probe Structure and Dynamics in Metal Ion–Molecule Complexes. *Int. Rev. Phys. Chem.* **2003**, 22, 407–435.
- (59) Duncan, M. A. Metal Cation Coordination and Solvation Studied with Infrared Spectroscopy in the Gas Phase. In *Physical Chemistry of Cold Gas Phase Functional Molecules and Clusters*; Ebata, T., Fujii, M., Eds.; Springer: Berlin, 2019; pp 157–194.
- (60) Frisch, M. J.; Trucks, G. W.; Schlegel, H. B.; Scuseria, G. E.; Robb, M. A.; Cheeseman, J. R.; Scalmani, G.; Barone, V.; Mennucci, B.; Petersson, G. A.; et al. *Gaussian09*, Revision D.01; Gaussian, Inc.: Wallingford, CT, 2009.
- (61) Weigend, F.; Ahlrichs, R. Balanced Basis Sets of Split Valence, Triple Zeta Valence and Quadruple Zeta Valence Quality for H to Rn: Design and Assessment for Accuracy. *Phys. Chem. Chem. Phys.* **2005**, 7, 3297–3305.
- (62) Shimanouchi, T. Molecular Vibrational Frequencies. In NIST Chemistry WebBook, NIST Standard Reference Database Number 69; Linstrom, P. J., Mallard, W. G., Eds.; National Institute of Standards and Technology: Gaithersburg, MD, 20899 (http://webbook.nist.gov).
- (63) Harvey, J. N. DFT Computation of Relative Spin-State Energetics of Transition Metal Compounds. *Struct. Bonding (Berlin, Ger.)* **2004**, *112*, 151–184.
- (64) Cramer, C. J.; Truhlar, D. J. Density Functional Theory for Transition Metals and Transition Metal Chemistry. *Phys. Chem. Chem. Phys.* **2009**, *11*, 10757–10816.
- (65) Cohen, A. J.; Mori-Sanchez, P.; Yang, W. Challenges for Density Functional Theory. *Chem. Rev.* **2012**, *112*, 289–320.
- (66) Fraser, G. T.; Suenram, R. D.; Lovas, F. J.; Pine, A. S.; Hougen, J. T.; Lafferty, W. J.; Muenter, J. S. Infrared and Microwave Investigations of Interconversion Tunneling in the Acetylene Dimer. *J. Chem. Phys.* **1988**, *89*, 6028–6045.
- (67) Shuler, K.; Dykstra, C. E. Interaction Potentials and Vibrational Effects in the Acetylene Dimer. *J. Phys. Chem. A* **2000**, *104*, 4562–4570.
- (68) Okumura, M.; Yeh, L. I.; Myers, J. D.; Lee, Y. T. Infrared Spectra of the Cluster Ions H₇O₃⁺-H₂ and H₉O₄⁺-H₂. *J. Chem. Phys.* **1986**, *85*, 2328–2329.
- (69) Yeh, L. I.; Okumura, M.; Myers, J. D.; Price, J. M.; Lee, Y. T. Vibrational Spectroscopy of the Hydrated Hydronium Cluster Ions $H_3O^+(H_2O)_n$ (n = 1, 2, 3). *J. Chem. Phys.* **1989**, *91*, 7319–7330.
- (70) Ebata, T.; Fujii, A.; Mikami, N. Vibrational Spectroscopy of Small-sized Hydrogen-bonded Clusters and their Ions. *Int. Rev. Phys. Chem.* **1998**, *17*, 331–361.
- (71) Bieske, E. J.; Dopfer, O. High-resolution Spectroscopy of Cluster Ions. *Chem. Rev.* **2000**, *100*, 3963–3998.
- (72) Robertson, W. H.; Johnson, M. A. Molecular Aspects of Halide Hydration: The Cluster Approach. *Annu. Rev. Phys. Chem.* **2003**, *54*, 173–213.
- (73) Zhao, Z.; Kong, X.; Yang, D.; Yuan, Q.; Xie, H.; Fan, H.; Zhao, J.; Jiang, L. Reactions of Copper and Silver Cations with Carbon Dioxide: An Infrared Photodissociation Spectroscopic and Theoretical Study. *J. Phys. Chem. A* **2017**, *121*, 3220–3226.
- (74) Kocak, A.; Ashraf, M. A.; Metz, R. B. Vibrational Spectroscopy Reveals Varying Structural Motifs in $Cu^+(CH_4)_n$ and $Ag^+(CH_4)_n$ (n = 1–6). *J. Phys. Chem. A* **2015**, *119*, 9653–9665.
- (75) Carvajal, M. A.; Novoa, J. J.; Alvarez, S. Choice of Coordination Number in d¹⁰ Complexes of Group 11 Metals. *J. Am. Chem. Soc.* **2004**, *126*, 1465–1477.